Understanding the shape of the galaxy two-point correlation function at $z \simeq 1$ in the COSMOS field

S. de la Torre,[2,3][*] L. Guzzo,[2] K. Kovač,[8] C. Porciani,[4] U. Abbas,[7] B. Meneux,[5,6]
C.M. Carollo,[8] T. Contini,[9] J.-P. Kneib,[1] O. Le Fèvre,[1] S.J. Lilly,[8] V. Mainieri,[10]
A. Renzini,[11] D. Sanders,[21] M. Scodeggio,[3] N. Scoville,[22] G. Zamorani,[12] S. Bardelli,[12]
M. Bolzonella,[12] A. Bongiorno,[5] K. Caputi,[8] G. Coppa,[12] O. Cucciati,[1] L. de Ravel,[1]
P. Franzetti,[3] B. Garilli,[3] A. Iovino,[2] P. Kampczyk,[8] C. Knobel,[8] A.M. Koekemoer,[13]
F. Lamareille,[9] J.-F. Le Borgne,[9] V. Le Brun,[1] C. Maier,[8] M. Mignoli,[12] R. Pelló,[9]
Y. Peng,[8] E. Perez-Montero,[9] E. Ricciardelli,[14] J. Silverman,[8] M. Tanaka,[10] L. Tasca,[3]
L. Tresse,[1] D. Vergani,[12] N. Welikala,[1] E. Zucca,[12] D. Bottini,[3] A. Cappi,[12]
P. Cassata,[15] A. Cimatti,[16] M. Fumana,[3] O. Ilbert,[1] A. Leauthaud,[17] D. Maccagni,[3]
C. Marinoni,[18] H.J. McCracken,[19] P. Memeo,[3] P. Nair,[12] P. Oesch,[8] L. Pozzetti,[12]
V. Presotto,[2] and R. Scaramella[20]

[1] *Laboratoire d'Astrophysique de Marseille, Marseille, France*
[2] *INAF - Osservatorio Astronomico di Brera, Milano, Italy*
[3] *INAF - Istituto di Astrofisica Spaziale e Fisica Cosmica di Milano, Milano, Italy*
[4] *Argelander Institute for Astronomy, University of Bonn, Bonn, Germany*
[5] *Max Planck Institut für Extraterrestrische Physik, Garching, Germany*
[6] *Universitats-Sternwarte, Muenchen, Germany*
[7] *INAF - Osservatorio Astronomico di Torino, Pino Torinese, Italy*
[8] *Institute of Astronomy, ETH Zurich, Zurich, Switzerland*
[9] *Laboratoire d'Astrophysique de l'Observatoire Midi-Pyrénées, Toulouse, France*
[10] *European Southern Observatory, Garching, Germany*
[11] *INAF - Osservatorio Astronomico di Padova, Padova, Italy*
[12] *INAF - Osservatorio Astronomico di Bologna, Bologna, Italy*
[13] *Space Telescope Science Institute, Baltimore, USA*
[14] *Dipartimento di Astronomia, Universitá di Padova, Padova, Italy*
[15] *Department of Astronomy, University of Massachusetts, Amherst, USA*
[16] *Dipartimento di Astronomia, Universitá di Bologna, Bologna, Italy*
[17] *Berkeley Lab & Berkeley Center for Cosmological Physics, University of California, Berkeley, USA*
[18] *Centre de Physique Théorique de Marseille, Marseille, France*
[19] *Institut d'Astrophysique de Paris, Paris, France*
[20] *INAF - Osservatorio Astronomico di Roma, Roma, Italy*
[21] *Institute for Astronomy, University of Hawaii, Honolulu, USA*
[22] *Astronomy Department, Caltech, Pasadena, USA*

ABSTRACT

We investigate how the shape of the galaxy two-point correlation function as measured in the zCOSMOS survey depends on local environment, quantified in terms of the density contrast on scales of $5\,h^{-1}$ Mpc. We show that the flat shape previously observed at redshifts between $z = 0.6$ and $z = 1$ can be explained by this volume being simply 10% over-abundant in high-density environments, with respect to a Universal density probability distribution function. When galaxies corresponding to the top 10% tail of the distribution are excluded, the measured $w_p(r_p)$ steepens and becomes indistinguishable from ΛCDM predictions on all scales. This is the same effect recognised by Abbas & Sheth in the SDSS data at $z \simeq 0$ and explained as a natural consequence of halo-environment correlations in a hierarchical scenario. Galaxies living in high-density regions trace dark matter halos with typically higher masses, which are more correlated. If the density probability distribution function of the sample is particularly rich in high-density regions because of the variance introduced by its finite size,

1 INTRODUCTION

Advances in the spectroscopic survey capabilities of 8-meter class telescopes have allowed us in the recent years to extend detailed studies of the clustering of galaxies to the $z \simeq 1$ Universe (Coil et al. 2004; Le Fèvre et al. 2005; Pollo et al. 2006; Coil et al. 2006; Meneux et al. 2006; de la Torre et al. 2007; Meneux et al. 2008; Coil et al. 2008; Abbas et al. 2010). The most recent contribution to this endeavour is the COSMOS survey (Scoville et al. 2007), and in particular zCOSMOS, its redshift follow-up with VIMOS at the ESO-VLT (Lilly et al. 2007).

Early angular studies of the COSMOS field (McCracken et al. 2007) and more recent analyses of the first ten thousand zCOS-MOS redshifts to $I_{AB} = 22.5$, have evidenced significant "excess" clustering in the large-scale shape of the two-point angular and projected correlation function. The redshift information from zCOSMOS, in particular, shows this excess to dominate in the redshift range $0.5 < z < 1$ (Meneux et al. 2009). More precisely, the shape of the projected two-point correlation function $w_p(r_p)$ appears to decay much less rapidly than observed at similar redshifts in independent data as the VVDS survey (Meneux et al. 2008) and with respect to predictions of standard ΛCDM cosmology as incarnated by the Millennium simulation (De Lucia & Blaizot 2007; Kitzbichler & White 2007). The observed flat shape[1] is difficult to reconcile with the theory, unless an unrealistic scale-dependent bias between galaxies and matter is advocated. While plausibly related to the presence of particularly rich large-scale structures dominating the COSMOS volume around $z \simeq 0.7$ (e.g. Meneux et al. 2009; Guzzo et al. 2007), this effect still awaits a quantitative explanation.

In a recent series of papers, Abbas & Sheth (2005, 2006, 2007) have used the Sloan Digital Sky Survey (SDSS, York et al. 2000), together with *Halo Occupation Distribution* models (HOD, e.g. Cooray & Sheth 2002) to show how in general the amplitude and shape of the galaxy correlation function depend on the *environment* in which the galaxies are found. Once a local density is suitably defined over a given scale, galaxies living in over-dense regions show a stronger clustering than those in average or under-dense environments. This is shown to be a consequence of the direct correlation arising in hierarchical clustering between the mass of the dark matter halos in which galaxies are embedded, and their large-scale environment: the mass function of dark-matter halos is top-heavy in high-density regions, thus selecting galaxies in these environments we are selecting halos of higher mass, which are more clustered. The net result is to introduce a *scale-dependent bias* in the observed correlation function, when this is compared to the expected dark-matter clustering (Abbas & Sheth 2006, 2007).

In this Letter we investigate whether this effect is at work also at $z \simeq 0.7$ and could explain quantitatively the observed shape of $w_p(r_p)$ in the zCOSMOS data.

2 DATA AND METHODS

2.1 The zCOSMOS 10k-bright sample

zCOSMOS is a large spectroscopic survey performed with the VIsible Multi-Object Spectrograph (VIMOS, Le Fèvre et al. 2003) at the ESO–VLT. The zCOSMOS-bright survey (Lilly et al. 2007) has been designed to follow-up spectroscopically the entire 1.7 deg^2 COSMOS-ACS field (Scoville et al. 2007; Koekemoer et al. 2007) down to $I_{AB} = 22.5$. We use in this analysis the first-epoch set of redshifts, usually referred to as the *zCOSMOS 10k-bright sample* ("10k sample", hereafter), including 10, 644 galaxies. At this magnitude limit, the survey redshift distribution peaks at $z \simeq 0.6$, with a tail out to $z \simeq 1.2$. We only consider secure redshifts, i.e. confidence classes 4.x, 3.x, 9.3, 9.5, 2.4, 2.5, and 1.5, representing 88% of the full 10k sample (see Lilly et al. 2009, for details) and 20.4% of the complete $I_{AB} < 22.5$ magnitude-limited parent sample over the same area. These data are publicly available through the ESO Science Data Archive site[2].

2.2 Mock galaxy surveys

In addition to the observed data, in this analysis we also make use of a set of 24 mock realisations of the zCOSMOS survey, constructed combining the Millennium Run N-body simulation[3], with a semi-analytical recipe of galaxy formation (De Lucia & Blaizot 2007). The Millennium Run is a large dark matter N-body simulation that follows the hierarchical evolution of 2160^3 particles between $z = 127$ and $z = 0$ in a cubic volume of $500^3 \ h^{-3} \ Mpc^3$. It assumes a concordance cosmological ΛCDM model with $(\Omega_m, \ \Omega_\Lambda, \ \Omega_b, \ h, \ n, \ \sigma_8) = (0.25, \ 0.75, \ 0.045, \ 0.73, \ 1, \ 0.9)$. The resolution of the N-body simulation, $8.6 \times 10^8 \ h^{-1} M_\odot$, coupled with the semi-analytical model allows one to resolve with a minimum of 100 particles halos containing galaxies with a luminosity of $0.1L^*$ (see Springel et al. 2005). Galaxies are generated inside these dark matter halos using the semi-analytic model of Croton et al. (2006), as improved by De Lucia & Blaizot (2007). This model includes the physical processes and requirements originally introduced by White & Frenk (1991) and refined by Kauffmann & Haehnelt (2000), Springel et al. (2001), De Lucia et al. (2004), and Springel et al. (2005). Twenty-four mocks are created, and then "observed" as to reproduce the zCOSMOS selection function (Iovino et al. 2010).

2.3 Local density estimator

To characterise galaxy environment we use the dimensionless density contrast measured by Kovač et al. (2010) around each galaxy in the sample. For each galaxy at a comoving position $\mathbf{r}$ we compute the dimensionless 3D density contrast smoothed on a scale R, $\delta_g(\mathbf{r}, R) = (\rho(\mathbf{r}, R) - \bar{\rho}(\mathbf{r}))/\bar{\rho}(\mathbf{r})$, where $\rho(\mathbf{r}, R)$ is the density of galaxies measured on a scale R and $\bar{\rho}(\mathbf{r})$ is the overall mean density at $\mathbf{r}$. $\rho(\mathbf{r}, R)$ is estimated around each galaxy of the sample by counting objects within an aperture (defined either through a top-hat of size R or a Gaussian filter with similar dispersion). The reconstructed over-densities are properly corrected for the survey selection function and edge effects. Kovač et al. (2010) studied different density estimators, corresponding to varying galaxy tracers, filter shapes and smoothing scales. Here we use δ_g as reconstructed with a Gaussian filter with dispersion $R = 5 \, h^{-1}$ Mpc. Note that the mass enclosed by such filter is equal to that inside a top-hat filter of size $\sim 7.8 \, h^{-1}$ Mpc. We refer the reader to Kovač et al. (2010) for a full description of the technique.

---

[1] $\gamma \sim 1.5$ instead of the $\gamma \sim 1.8$ expected when approximating $\xi(r)$ with a power law (i.e. $\xi(r) = (r_0/r)^\gamma$) below $r = 10 \, h^{-1}$ Mpc

[2] http://archive.eso.org/cms/eso-data/data-packages/
[3] http://www.mpa-garching.mpg.de/millennium/

2.4 Expected probability distribution function of the density contrast

The density contrast distribution can be predicted analytically using some approximations. Empirically, it has been found that the probability distribution function (PDF) of the mass density contrast in real (comoving) space smoothed on a scale R is well described by a lognormal distribution (Coles & Jones 1991),

$$P(\delta) = \frac{(2\pi\omega_R^2)^{-1/2}}{1+\delta} \exp\left(-\frac{(\ln(1+\delta)+\omega_R^2)^2}{2\omega_R^2}\right) \ , \qquad (1)$$

where $\omega_R^2 = \ln(1 + \langle\delta^2\rangle_R)$ and $\langle\delta^2\rangle_R = \sigma_R^2(z)$, with $\sigma_R(z)$ being the standard deviation of mass fluctuations at redshift z on the same scale:

$$\sigma_R^2(z) = \int_0^\infty \frac{dk}{k} \frac{k^3 P(k,z)}{2\pi^2} |W(kR)|^2 \ . \qquad (2)$$

Here $P(k,z)$ is the mass power spectrum at redshift z in the adopted cosmology and $W(x)$ is the Fourier transform of the smoothing window function. For our purpose we use the mass power spectrum of Smith et al. (2003), which includes the non-linear evolution of the initial mass fluctuations field.

The density field recovered from redshift surveys is affected by galaxy peculiar motions. Therefore one needs to convert the real-space PDF model into redshift-space in order to be able to compare it to observations. It has been found that the redshift-space PDF of the density contrast is still well described by a lognormal distribution (Sigad et al. 2000), with a standard deviation $\sigma_R^z(z)$ related to that in real space as (Kaiser 1987),

$$\sigma_R^z(z) = \left(1 + \frac{2}{3}f(z) + \frac{1}{5}f^2(z)\right)^{\frac{1}{2}} \sigma_R(z) \ . \qquad (3)$$

Here σ_R and σ_R^z are respectively the real- and redshift-space standard deviations and $f(z)$ denotes the growth rate of structure, which in the framework of General Relativity is well approximated as $f(z) \simeq \Omega_m^{0.55}(z)$ (Wang & Steinhardt 1998).

Following this procedure we obtain the PDF of the mass density contrast in redshift-space. To obtain that of galaxies we have to further apply a biasing factor. For our purposes here, we simply assume linear deterministic biasing, setting $\delta_g = b\delta$ (however, see Marinoni et al. 2005). We choose a value $b = \sqrt{2.05}$, as required to match the large-scale amplitude of the two-point correlation function of galaxies in our sample, as we shall show in Sec. 3.

By definition, the PDF described by equation 1 refers to the distribution of δ as measured in randomly placed spheres within the survey volume. On the other hand, for the data we have at our disposal only the *conditional* values of δ_g as measured in volumes centred on each galaxy in the sample. Given the probabilistic meaning of the distribution function of the density $\mathcal{P}(\rho)$ in the two cases they must be related as

$$\mathcal{P}_c(\rho) = \frac{\rho\mathcal{P}(\rho)}{\displaystyle\int_0^\infty \rho\mathcal{P}(\rho)d\rho} = \frac{\rho}{\bar{\rho}}\mathcal{P}(\rho) \ . \qquad (4)$$

Being $P(\delta) = \bar{\rho}\mathcal{P}(\rho)$, the corresponding relation between the PDFs of the density contrast $P(\delta)$ is

$$P_c(\delta) = \frac{(1+\delta)P(\delta)}{\overline{1+\delta}} \ , \qquad (5)$$

where $\overline{1+\delta} = 1$.

We are then in the position to compare the theoretically predicted P_c (normalised to the total number of galaxies in the sample) to the observed distribution. This is presented in Fig. 1, together with the mean and scatter (68% confidence corridor) of the 24 mock samples. The analytical prediction and the mean of the mocks are in fair agreement (although they disagree in the details at the 1σ level). Note, however, that the detailed shape and amplitude of the analytical prediction are quite sensitive to the choice of the effective redshift $\bar{z}$ of the survey. Here we have used the mean value $\bar{z} \simeq 0.56$ yielded by the actual redshift distribution dN/dz of the survey, but using e.g. $\bar{z} \simeq 0.6$ would give a better agreement with the PDF from the simulations. Additionally, the analytical prediction cannot include the small scale "Finger-of-God" effect due to high velocities in clusters (which however has the effect to reduce power on small scales). Finally, it has been computed using the more up-to-date $\sigma_8 = 0.8$, to check the impact of the value $\sigma_8 = 0.9$ used for the Millennium Run. Beyond these points, the simple goal of the analytical model is to show an alternative – yet more idealised – example, in addition to the mocks, of what one should expect from the theory. What is relevant for this work is that the conditional PDF of the data differs strongly from both theoretical predictions. Peaking at $\delta_g \simeq -0.2$, it shows an extended high-density tail out to $\delta_g \simeq 7$. The distribution expected from the models is more peaked around $\delta_g = 0$ and drops more rapidly for $\delta_g > 2$. This plot clearly shows a statistically significant excess of high-density regions in the galaxy data. [4]

2.5 Clustering estimation

We estimate real-space galaxy clustering using the standard projected two-point correlation function, $w_p(r_p)$, that properly corrects for redshift-space distortions due to galaxy peculiar motions. This is obtained by projecting the two-dimensional two-point correlation function $\xi(r_p, \pi)$ along the line-of-sight[5]

$$w_p(r_p) = 2\int_0^\infty \xi(r_p,\pi)d\pi \ , \qquad (6)$$

where r_p and π are the components of the galaxy-galaxy separation vector respectively perpendicular and parallel to the line-of-sight (Peebles 1980; Fisher et al. 1994). $\xi(r_p,\pi)$ is measured using the Landy & Szalay (1993) estimator and properly accounting for the survey selection function and various incompleteness effects, as thoroughly described in de la Torre et al. (2009). Error bars are estimated through the blockwise bootstrap method (e.g. Porciani & Giavalisco 2002; Norberg et al. 2009). This is discussed in detail and compared to results from mock samples in Meneux et al. (2009) and Porciani et al. (2010). All clustering codes and methods used here have been extensively tested against independent programs in the course of the latter analyses.

---

[4] An ongoing analysis of the fuller COSMOS sample to $I_{AB} = 24$ based on photometric redshifts (Scoville et al. 2010, in preparation), seems to indicate a better agreement of the observed PDF to that of the Millennium mocks. This might be explained as a consequence of the larger volume of the sample used (lower cosmic variance), together with the fairly large smoothing window used to define the over-densities and, most importantly, the blurring of the PDF produced by the photometric redshift errors.

[5] In practice, a finite value for the the upper integration limit is adopted. We use $20\,h^{-1}$ Mpc which recovers the signal dispersed by redshift distortions, while minimising the noise that dominates at large values of π (see also Meneux et al. 2009; Porciani et al. 2010).
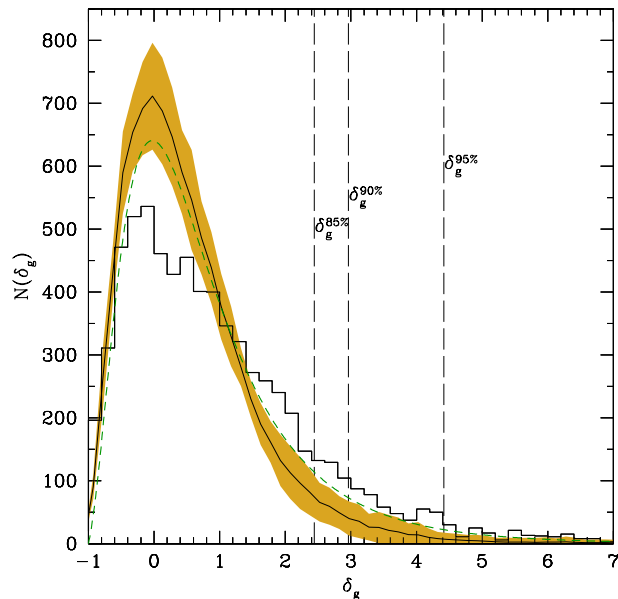
Figure 1. The probability distribution function of the density contrast, measured around each galaxy in the current zCOSMOS 10k catalogue as discussed in the text (histogram). The solid line and shaded area correspond respectively to the mean and 1σ dispersion of the same statistics, measured on the 24 Millennium mocks; the dashed curve gives instead, as reference, the expected theoretical distribution for a lognormal model in a ΛCDM cosmology with $(\Omega_m, \Omega_\Lambda, \sigma_8) = (0.25, 0.75, 0.8)$, at the mean redshift of the 10k sample, computed as discussed in the text. The vertical solid lines correspond to values of the density contrast excluding the top 5%, 10% and 15% of the distribution.

3   RESULTS AND DISCUSSION

In Fig. 2 we show the projected correlation function $w_p(r_p)$ computed for the 10k sample in the redshift range $0.6 < z < 1$ (top curve), together with those from a series of sub-samples in which we gradually eliminated galaxies located in the most dense environments. We excluded, respectively, the top 5%, 10%, and 15% fractions of the distribution of over-densities, corresponding to the dashed vertical lines in Fig. 1. $w_p(r_p)$ for the full 10k sample shows a very flat shape, with significant "excess clustering" above $1\,\mathrm{h}^{-1}$ Mpc, as seen in previous analyses of the COSMOS/zCOSMOS data. When galaxies in the densest environments are excluded, however, the large-scale "shoulder" gradually disappears. What we see is a clear dependence of the mean large-scale clustering of galaxies on the type of environments they inhabit, similarly to the results of Abbas & Sheth (2007) from the SDSS.

In the same figure we also show the "universal" $w_p(r_p)$ expected in the standard ΛCDM cosmological model with linear biasing. The theory predictions are, again, obtained in two ways. First, we use *HALOFIT* (Smith et al. 2003) to compute directly the approximated non-linear mass power spectrum expected at the survey mean redshift. Secondly, we compute the average and scatter of $w_p(r_p)$ from the 24 mock samples. Remarkably, the two curves (solid and dashed black lines) are virtually indistinguishable above $1\,\mathrm{h}^{-1}$ Mpc once the *HALOFIT* mass correlation function is properly multiplied by an arbitrary linear bias factor of $b^2 = 2.05$. The comparison to the data shows a very good agreement for the 10k sub-sample in which the 10% densest environments were excluded. We note that the shape of $w_p(r_p)$ measured from the independent
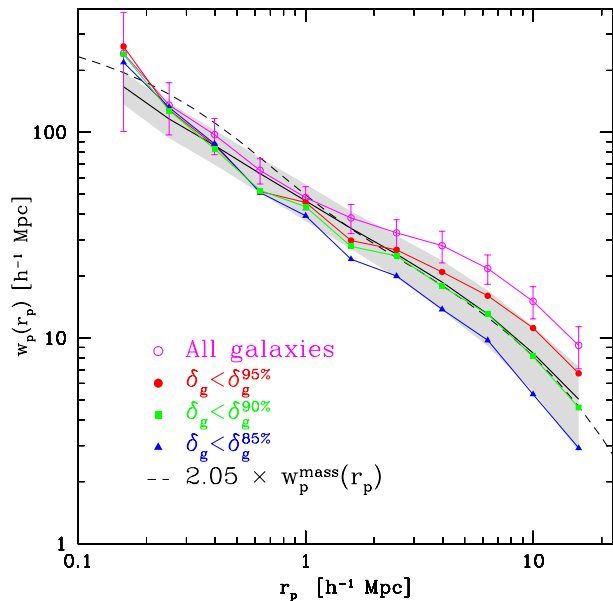
Figure 2. The projected two-point correlation function $w_p(r_p)$ of the zCOSMOS 10k at $0.6 < z < 1$, compared to sub-samples in which galaxies living in the densest environments are gradually excluded (top to bottom). To reduce confusion, error bars are shown for the main sample only, being in general of amplitude comparable to the scatter of the mock samples indicated by the shaded area. The thick solid line and surrounding shaded corridor correspond in fact to the mean and 1σ scatter of the 24 mock surveys. For comparison, the dashed curve also shows the *HALOFIT* (Smith et al. 2003) analytic prescription for the non-linear mass power spectrum (assuming ΛCDM with $(\Omega_m, \Omega_\Lambda, \sigma_8) = (0.25, 0.75, 0.8)$), multiplied by an arbitrary linear bias $b^2 = 2.05$. The shape of $w_p(r_p)$ for zCOSMOS galaxies agrees with the models when the 10% densest environments are eliminated.

VVDS survey shows a shape which is closer to the model predictions (Meneux et al. 2009). With this thresholding in density of the 10k data, therefore, we are able to bring the measured shape of galaxy clustering at $z \simeq 0.7$ from zCOSMOS, VVDS and the standard cosmological model within close agreement, suggesting a more quantitative interpretation of the flat shape of $w_p(r_p)$ observed in zCOSMOS at these redshifts. In previous papers (e.g. Meneux et al. 2009; Kovac et al. 2009) we already suggested that this could be due to the presence of particularly significant large-scale structures between $z = 0.5$ and $z = 1$. Here we see that it is in fact driven by an excess of galaxies sampling high-density regions, skewing the density distribution away from the supposedly "Universal". Fig. 3 shows where these high-density galaxies are actually located within the 10k sample. The galaxies belonging to the 10% high-density tail are marked by (red) circles and turn out to belong to a few very well-defined structures only.[6] It is easy to imagine that if embedded in a larger volume, these structures would not weight so much as to modify significantly the overall shape of the PDF. As seen from the histogram in Fig. 1, however, in this vol-

---

[6] We also directly tested whether the two-point correlation functions computed on the density-thresholded samples were by any means sensitive to the way the "depleted" sub-volumes were treated (e.g. kept in or excluded when building the standard reference random sample); no significant changes were found.
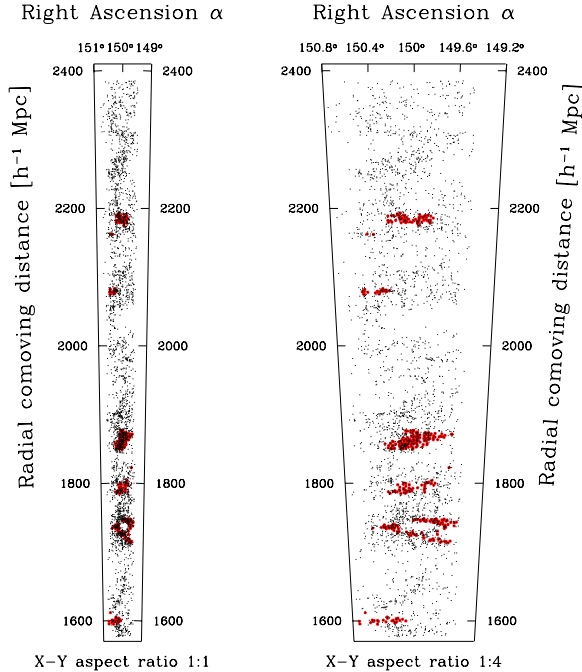
Figure 3. The spatial distribution of galaxies with $0.6 < z < 1$ (dots) in the zCOSMOS 10k sample, highlighting those inhabiting the 10% highest-density tail of the distribution (circles). These galaxies clearly belong to a few well-defined structures. The right-hand plot is simply an expanded version of the pencil-beam on the left, to enhance visibility.

ume there is a clear over-abundance of high-density galaxy environments, while regions with average density are under-represented.

One may wonder however, whether the theoretical model represented by the Millennium mocks can be taken as a reliable reference. In fact, it has been shown that this specific model tends to overestimate the overall amplitude of $w_p(r_p)$ at $z \simeq 1$ and does not reproduce the observed clustering segregation in colour (e.g. Coil et al. 2008; de la Torre et al., in preparation) In general, semi-analytical recipes do tend to affect the amplitude and shape of the correlation function. This however happens only on small scales, where the complex interplay between galaxy formation processes and the distribution of dark-matter halos has an impact. On large scales instead, they predict a fairly linear biasing, as we can see directly comparing the solid and dashed black lines in Fig. 2. This means that the large-scale shape of the correlation function is essentially driven by the underlying mass distribution in the assumed cosmological model and not by the details of the semi-analytic recipe adopted to generate galaxies. A different recipe would not affect, therefore, the results obtained here, unless we postulate the existence of dramatically non-local galaxy formation processes (e.g. Narayanan et al. 2000).

We also note from Fig. 2 that the dependence of $w_p(r_p)$ on the PDF threshold is essentially on large scales. Below $\sim 1\,\mathrm{h}^{-1}$ Mpc there is no significant change when denser and denser environments are excluded. In their analysis of the SDSS Abbas & Sheth (2007) consider sub-samples defined as extrema of the density distribution, i.e. using galaxies lying on the tails of the distribution on both sides. With this selection, they find a change in $w_p(r_p)$ for different environments also on small scales. It can be shown simply using the conservation of galaxy pairs (see Eq. 1 of Abbas &

Sheth 2007) that the two results are in fact consistent with each other (Ravi Sheth, private communication).

These results highlight the importance in redshift surveys of an accurate reconstruction of the density field, to evidence possible peculiarities in the overall PDF as sampled by that specific catalogue. Further strengthening the results obtained by Abbas & Sheth (2007) at $z \simeq 0$, we have shown that an anomalous density distribution function can significantly bias the recovered two-point correlation function, making it difficult to draw general conclusions from its shape. This result provides another example of the intrinsic difficulty existing when comparing observations of the galaxy distribution to theoretical predictions. The theory provides us with fairly accurate forecasts for the distribution of the dark matter and for that of the halos within which we believe galaxies form (e.g. Mo et al. 1996; Sheth & Tormen 1999). However, translating galaxy clustering measurements into constraints for the halo clustering involves understanding how the selected galaxies populate halos with different mass. The result presented here show how a sample particularly rich in dense structures favours higher-mass halos, which in turn are more clustered, thus biasing the observed correlation function as a function of scale. A more detailed analysis of the environmental dependence of galaxy clustering in the zCOSMOS-Bright sample and related HOD modelling will be presented in a future paper.

REFERENCES

Abbas, U., de La Torre, S., Le Fèvre, O., et al. 2010, MNRAS, 782
Abbas, U. & Sheth, R. K. 2005, MNRAS, 364, 1327
Abbas, U. & Sheth, R. K. 2006, MNRAS, 372, 1749
Abbas, U. & Sheth, R. K. 2007, MNRAS, 378, 641
Coil, A. L., Davis, M., Madgwick, D. S., et al. 2004, ApJ, 609, 525
Coil, A. L., Newman, J. A., Cooper, M. C., et al. 2006, ApJ, 644, 671
Coil, A. L., Newman, J. A., Croton, D., et al. 2008, ApJ, 672, 153
Coles, P. & Jones, B. 1991, MNRAS, 248, 1

Cooray, A. & Sheth, R. 2002, Phys. Rep., 372, 1

Croton, D. J., Springel, V., White, S. D. M., et al. 2006, MNRAS, 365, 11

de la Torre, S., Le Fèvre, O., Arnouts, S., et al. 2007, A&A, 475, 443

de la Torre, S., Le Fèvre, O., Porciani, C., et al. 2009, preprint (astro-ph/1003.6129)

De Lucia, G. & Blaizot, J. 2007, MNRAS, 375, 2

De Lucia, G., Kauffmann, G., & White, S. D. M. 2004, MNRAS, 349, 1101

Fisher, K. B., Davis, M., Strauss, M. A., Yahil, A., & Huchra, J. P. 1994, MNRAS, 267, 927

Guzzo, L., Cassata, P., Finoguenov, A., et al. 2007, ApJS, 172, 254

Iovino, A., Cucciati, O., Scodeggio, M., et al. 2010, A&A, 509, A40+

Kaiser, N. 1987, MNRAS, 227, 1

Kauffmann, G. & Haehnelt, M. 2000, MNRAS, 311, 576

Kitzbichler, M. G. & White, S. D. M. 2007, MNRAS, 376, 2

Koekemoer, A. M., Aussel, H., Calzetti, D., et al. 2007, ApJS, 172, 196

Kovac, K., Porciani, C., Lilly, S. J., et al. 2009, preprint (astro-ph/0910.0004)

Kovač, K., Lilly, S. J., Cucciati, O., et al. 2010, ApJ, 708, 505

Landy, S. D. & Szalay, A. S. 1993, ApJ, 412, 64

Le Fèvre, O., Guzzo, L., Meneux, B., et al. 2005, A&A, 439, 877

Le Fèvre, O., Saisse, M., Mancini, D., et al. 2003, in Proc. SPIE, ed. M. Iye & A. F. M. Moorwood, Vol. 4841, 1670–1681

Lilly, S. J., Le Brun, V., Maier, C., et al. 2009, ApJS, 184, 218

Lilly, S. J., Le Fèvre, O., Renzini, A., et al. 2007, ApJS, 172, 70

Marinoni, C., Le Fèvre, O., Meneux, B., et al. 2005, A&A, 442, 801

McCracken, H. J., Peacock, J. A., Guzzo, L., et al. 2007, ApJS, 172, 314

Meneux, B., Guzzo, L., de la Torre, S., et al. 2009, A&A, 505, 463

Meneux, B., Guzzo, L., Garilli, B., et al. 2008, A&A, 478, 299

Meneux, B., Le Fèvre, O., Guzzo, L., et al. 2006, A&A, 452, 387

Mo, H. J., Jing, Y. P., & White, S. D. M. 1996, MNRAS, 282, 1096

Narayanan, V. K., Berlind, A. A., & Weinberg, D. H. 2000, ApJ, 528, 1

Norberg, P., Baugh, C. M., Gaztañaga, E., & Croton, D. J. 2009, MNRAS, 396, 19

Peebles, P. J. E. 1980, The large-scale structure of the universe (Princeton University Press, 1980. 435 p.)

Pollo, A., Guzzo, L., Le Fèvre, O., et al. 2006, A&A, 451, 409

Porciani, C. & Giavalisco, M. 2002, ApJ, 565, 24

Porciani, C. et al. 2010, in preparation

Scoville, N., Aussel, H., Brusa, M., et al. 2007, ApJS, 172, 1

Sheth, R. K. & Tormen, G. 1999, MNRAS, 308, 119

Sigad, Y., Branchini, E., & Dekel, A. 2000, ApJ, 540, 62

Smith, R. E., Peacock, J. A., Jenkins, A., et al. 2003, MNRAS, 341, 1311

Springel, V., White, S. D. M., Jenkins, A., et al. 2005, Nature, 435, 629

Springel, V., White, S. D. M., Tormen, G., & Kauffmann, G. 2001, MNRAS, 328, 726

Wang, L. & Steinhardt, P. J. 1998, ApJ, 508, 483

White, S. D. M. & Frenk, C. S. 1991, ApJ, 379, 52

York, D. G., Adelman, J., Anderson, Jr., J. E., et al. 2000, AJ, 120, 1579